JOURNAL OF MOLECULAR SPECTROSCOPY 161, 445–454 (1993)

Fourier Transform Emission Spectroscopy of the $A^6\Sigma^+$–$X^6\Sigma^+$ System of CrH: Evidence for a $^4\Sigma^+$ Lowest Excited State

R. S. RAM, C. N. JARMAN, AND P. F. BERNATH

Department of Chemistry, University of Arizona, Tucson, Arizona 85721; and Department of Chemistry, University of Waterloo, Waterloo, Ontario, Canada N2L 3G1

The emission spectrum of CrH has been observed in the near-infrared region from 10 000–13 500 cm^{-1} using a Fourier transform spectrometer. Compared with the previous work on this molecule, the present spectra provide greatly improved measurements of the line positions of the $A^6\Sigma^+$–$X^6\Sigma^+$ electronic transition. The rotational analysis of the 0 − 0 band has been performed providing the following principal molecular constants: T_{00} = 11 552.6848(10) cm^{-1}, B' = 5.271996(29) cm^{-1}, and B'' = 6.1317406(19) cm^{-1}. As was first noted by Kleman and Uhler, the excited state is perturbed. By correcting a few misassignments in the previous work, we conclude that a nearby $a^4\Sigma^+$ state is responsible for the perturbation. The $a^4\Sigma^+$ state has an approximate band origin T_{00} = 11 186 cm^{-1} and a preliminary rotational constant B_0 = 6.10 cm^{-1}. This state lies below the $A^6\Sigma^+$ state and is, therefore, the lowest lying excited state.

INTRODUCTION

Of all of the transition metal hydrides, CrH is the best characterized. A band at 3680 Å attributed to CrH was first observed by Gaydon and Pearse (*1*) in 1937. This ultraviolet system was later observed by O'Connor (*2*), Smith (*3*), and Kleman and Liljeqvist (*4*), but no analysis has been published.

Kleman and Liljeqvist (*4*) noted two additional transitions of CrH near 3290 and 8611 Å. The 0 − 0 and 0 − 1 bands of the near-infrared transition (A–X) were rotationally analyzed by Kleman and Uhler (*5*). O'Connor (*6*) analyzed the 1 − 0 and 1 − 1 bands of this transition of CrH as well as the corresponding 0 − 0 band of CrD.

Weltner and co-workers (*7, 8*) trapped CrH and CrD in an argon matrix and measured the electron spin resonance and the infrared spectra. These measurements confirmed the ground state as $X^6\Sigma^+$ and provided the hyperfine parameters.

More accurate ground state parameters were derived by the recent analysis of the pure rotational transitions of CrH by Corkery *et al.* (*9*). They measured the $N = 1 \leftarrow 0$ through $N = 5 \leftarrow 4$ transitions by far-infrared laser magnetic resonance.

Mid-infrared laser magnetic resonance was used to detect the vibration–rotation transitions of CrH (*10*). Lipus *et al.* (*10*) measured both the fundamental vibrational band (1-0) and the first hot band (2 − 1).

The thermochemical properties of CrH have been determined by several groups (*11–13*). The most recent determination of the dissociation energy was made by Chen *et al.* (*13*). They found the dissociation energy to be 45 kcal/mole from the threshold for hydride (H^-) abstraction by a Cr^+ ion beam.

The dissociation energy and other molecular properties have been calculated by ab initio methods for the ground $X^6\Sigma^+$ state (*14–16*). In general the experimental and theoretical values are in good agreement.

0022-2852/93 $5.00

Miller *et al.* (*17*) have measured the photoelectron spectra of CrH^-. The CrH^- ground state was assigned as $^7\Sigma^+$ and the electron affinity of CrH was measured to be 0.563 eV (*17*). Lin and Ortiz's calculations (*18*) are in excellent agreement with these experiments. Interestingly Miller *et al.* (*17*) are unable to assign one peak in their CrH^- photoelectron spectrum. We believe this feature to be the new low-lying $a^4\Sigma^+$ state.

Like many metal hydrides, CrH is found in the spectra of the sun (*19*) and cool stars in general (*20*). Engvold *et al.* (*19*) identified CrH in the spectra of sunspots using the lines of the $A^6\Sigma^+$–$X^6\Sigma^+$ transition. Similarly Lindgren and Olofsson (*20*) found evidence for this transition in the spectra of S-type stars.

We have remeasured the $A^6\Sigma^+$–$X^6\Sigma^+$ transition of CrH and CrD by Fourier transform emission spectroscopy of a hollow cathode lamp. Our rotational analysis of the 0 – 0 vibrational band of this transition is reported here. By correcting a few misassigned lines in the F_1 and F_6 spin components in the previous analysis (*5*) we are able to assign the perturbing electronic state as a $^4\Sigma^+$ state which lies below the $A^6\Sigma^+$ state.

Very recently Dai and Balasubramanian (*21*) have (at our suggestion) completed a set of CAS-MCSCF followed by second-order CI (SOCI) ab initio calculations of the low-lying states of CrH. Their results are, in general, in good accord with our observations.

EXPERIMENTAL DETAILS

The emission spectrum of CrH was observed in the near-infrared region using the 1-m Fourier transform spectrometer associated with the McMath Solar Telescope of the National Solar Observatory at Kitt Peak. The spectrum was excited in a Cr hollow cathode discharge lamp. A mixture of 2.2 Torr of Ne and 50 mTorr of H_2 was flowed slowly through the lamp. The lamp was operated at 400 V and 362 mA of current. The spectrometer was operated with a $CuSO_4$ filter (OG 570) and photodiode detectors. The use of the OG 570 filter and the silicon photodiodes limited the observed spectral region to the 10 000–17 500 cm^{-1} interval. A total of 10 scans were coadded in approximately 1 hr of integration at a resolution of 0.02 cm^{-1}.

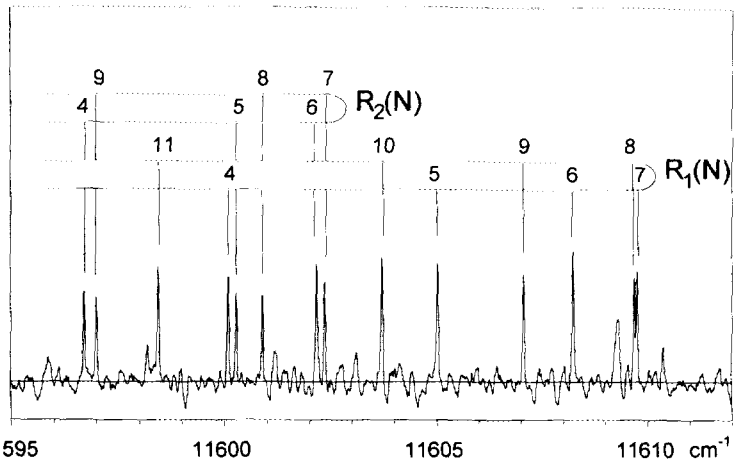

FIG. 1. A portion of the spectrum of CrH near the R_1 and R_2 heads of the 0 – 0 band of the $A^6\Sigma^+$–$X^6\Sigma^+$ transition.

TABLE I

Matrix Elements for the Rotational Levels of a $^6\Sigma^+$ State

$\Sigma = \frac{1}{2}$	$\Sigma = \frac{3}{2}$	$\Sigma = \frac{5}{2}$
$E - 16/3\{\lambda + \lambda_D(z+9-x)\} + 10\{\Theta + \Theta_D(z+9-x)\}$ $-4\{\gamma_S x - \gamma_{SD}(12z+9-x(z+9))\}$ $+B(z+9-x) - D(z^2+35z+90-2x(z+9))$ $+H(z^3+78z^2+697z+972-x(3z^2+79z+252))$ $+L(z^4+138z^3+2649z^2+11384z+11016-4x(z^3+52z^2+461z+810))$ $-\frac{1}{2}\begin{Bmatrix}+\gamma(17-x)+\gamma_D(34z+162-x(z+26))\\+\gamma_H(33z^2+707z+1530-6x(7z+51))\\+\gamma_L(41z^3+1838z^2+13009z+16524-3x(25z^2+509z+1428))\end{Bmatrix}$	$\sqrt{8z}\begin{Bmatrix}+10/3\lambda_D+5/2\Theta_D-3/2\gamma_S-\gamma_{SD}/4(6(z+7)-11x)\\-B+D(2(z+7)-x)-H(3z^2+64z+145-x(3z+23))\\-L(4z^3+172z^2+1172z+1532-x(6z^2+122z+352))\\+\frac{1}{2}\begin{Bmatrix}+\gamma\\+\gamma_D(z+22-x)\\+\gamma_H/2(2z^2+123z+505-2x(z+24))\\+\gamma_L/2\begin{pmatrix}2z^3+237z^2+2844z+5177\\-x(3z^2+182z+927)\end{pmatrix}\end{Bmatrix}\end{Bmatrix}$	$\sqrt{40z(z-3)}\begin{Bmatrix}-9/4\,\gamma_{SD}\\-D+H(3z+11-x)\\+L(6z^2+66z+112-4x(z+5))\\-\frac{1}{2}\begin{Bmatrix}+\gamma_D+\gamma_H/2(4z+38-x)\\+\gamma_L/2(6z^2+149z+391-3x(z+15))\end{Bmatrix}\end{Bmatrix}$
	$E - 4/3\{\lambda + \lambda_D(z+5)\} - 15\{\Theta + \Theta_D(z+5)\} - 18\gamma_{SD}(z-5)$ $+B(z+5) - D(z^2+23z+10) + H(z^3+54z^2+217z+20-8xz)$ $+L(z^4+98z^3+1049z^2+2000z+40-32xz(z+7))$ $-\frac{1}{2}\begin{Bmatrix}+13\gamma+\gamma_D(26z+50)+\gamma_H(39z^2+391z+100-8xz)\\+\gamma_L(52z^3+1264z^2+3716z+200-24xz(z+12))\end{Bmatrix}$	$\sqrt{5(z-3)}\begin{Bmatrix}-8/3\lambda_D+5\Theta_D+6\{\gamma_S+\gamma_{SD}(z+1)\}\\-B+D(2z+2)-H(3z^2+19z+4)\\-L(4z^3+64z^2+164z+8-8xz)\\+\frac{1}{2}\begin{Bmatrix}+\gamma+\gamma_D(2z+20)+\gamma_H(z^2+33z+20)\\+\gamma_L(z^3+69z^2+312z+40-8xz)\end{Bmatrix}\end{Bmatrix}$
		$E + 20/3\{\lambda + \lambda_D(z-3)\} + 5\{\Theta + \Theta_D(z-3)\} - 5\gamma/2$ $+(z-3)\begin{Bmatrix}+B-D(z+2)+H(z^2+9z+4)+L(z^3+21z^2+72z+8)\\-\frac{1}{2}\{2\gamma_D+\gamma_H(3z+4)+\gamma_L(4z^2+28z+8)\}-30\gamma_{SD}\end{Bmatrix}$

Note. $z = (J + \frac{3}{2})(J - \frac{1}{2})$, $x = \pm 3(J + \frac{1}{2})$. The upper and lower sign in the definition of x refer to the Wang sum and difference functions, which for a $^6\Sigma^+$ state give the e and f levels, respectively. If the state is regular, the Hund's case (a) basis correlates with the $e(F_1F_3F_5)$ and $f(F_2F_4F_6)$ Hund's case (b) labels for all J except for $J = \frac{3}{2}$ ($e(F_3F_5)$ and $f(F_4F_6)$) and $J = \frac{1}{2}$ ($e(F_5)$ and $f(F_6)$). Inverted states correlate with the $e(F_5F_3F_1)$ and $f(F_6F_4F_2)$ labels for all J. The matrices are symmetrical and only the upper triangle is shown.

TABLE II

Observed Transition Wavenumbers (in cm^{-1}) of the 0 − 0 Band of the A–X System of CrH

N	R1	O-C		P1	O-C		R2	O-C		P2	O-C		R3	O-C		P3	O-C	
0	11563.438	-5																
1	11575.125	4					11576.154	-5										
2	11585.136	9		11526.834	2		11584.601	0		11530.215	4		11580.333	-0				
3	11593.469	17	*	11513.804	6		11591.479	-5					11586.150	-1		11510.895	-4	
4	11600.100	25	*	11499.284	11		11596.724	-3		11498.950	3		11590.301	1		11494.365	0	
5	11605.024	37	*	11483.186	17	*	11600.291	-3		11481.364	-2		11592.745	10	*	11475.943	3	
6	11608.241	61	*	11465.485	29	*	11602.171	3		11462.251	-2		11593.469	21	*	11455.821	8	
7	11609.757	101	*	11446.171	41	*	11602.364	20	*	11441.572	1		11592.482	37	*	11434.049	12	*
8	11609.689	272	*	11425.261	62	*	11600.907	88	*	11419.318	3		11589.805	75	*	11410.660	20	*
9	11607.067	-405	*	11402.783	106	*	11597.009	-593	*	11395.508	20	*	11584.024	-1292	*			
10	11603.721	-109	*	11378.860	275	*	11592.553	-147	*	11370.198	92	*	11579.272	60	*	11359.159	75	*
11	11598.448	-55	*	11352.543	-399	*	11586.020	-107	*	11342.599	-589	*	11571.567	133	*	11329.688	-1287	*
12	11591.479	-29	*	11325.674	-103	*	11577.810	-86	*	11314.612	-149	*	11562.183	184	*	11301.412	62	*
13	11582.842	-18	*	11297.066	-49	*	11567.958	-68	*	11284.746	-104	*	11551.198	272	*	11270.363	125	*
14	11572.573	-9		11266.963	-25	*	11556.499	-39	*	11253.401	-86	*	11538.637	403	*	11237.862	190	*
15	11560.689	-3		11235.417	-12	*	11543.462	8	*	11220.636	-68	*	11524.513	566	*	11203.962	275	*
16	11547.214	-4		11202.468	-3		11528.901	102	*	11186.496	-41	*	11508.941	851	*	11168.713	396	*
17	11532.187	4		11168.155	1		11512.900	299	*	11151.029	7	*	11492.048	1357	*	11132.170	569	*
18	11515.619	1		11132.512	-1		11495.742	855	*	11114.299	99	*	11474.328	2551	*	11094.425	848	*
19	11497.548	-4		11095.590	1		11479.523	3833	*	11076.410	298	*	11459.016	7636	*	11055.639	1350	*
20	11478.018	1		11057.429	3		11452.167	-2877	*	11037.646	846	*	11425.748	-3785	*	11016.327	2551	*
21	11457.048	1					11431.267	-1716	*	11000.139	3829	*	11404.448	-1823	*	10979.720	7636	*
22	11434.672	-9		10977.559	4		11408.140	-1404	*	10951.799	-2888	*	11380.538	-1091	*	10925.474	-3787	*
23	11410.950	-3		10935.939	-1		11383.465	-1303	*	10910.260	-1720	*	11354.978	-669	*	10883.527	-1825	*
24				10893.274	4		11357.425	-1270	*	10866.823	-1415	*	11327.999	-367	*	10839.310	-1096	*
25	11359.562	-19		10849.595	1		11330.085	-1282	*	10822.213	-1300	*	11299.721	-107	*	10793.809	-667	*
26				10804.944	-21		11301.502	-1330	*	10776.584	-1273	*	11270.195	116	*	10747.246	-365	*
27				10759.434	-1		11271.729	-1407	*	10730.036	-1289	*				10699.759	-108	*
28				10713.059	-1					10682.651	-1321	*				10651.418	117	*
29				10665.899	1					10634.478	-1379	*				10602.386	418	*
30				10618.003	0					10585.646	-1392	*				10552.491	562	*
31										10536.025	-1552	*						

O-C: Observed minus calculated line positions in units of 10-3 cm-1.
*: Not included directly in the final fit. See text for detail.

In addition to the CrH molecular transitions, the spectrum also contained numerous Ne and Cr atomic lines. The measurements of the Ne atomic lines by Palmer and Engleman (*22*) were used to calibrate our spectra. The absolute accuracy of calibration of the wavenumber scale is expected to be better than ± 0.001 cm^{-1}. The CrH lines had a width of about 0.045 cm^{-1} and a maximum signal-to-noise ratio of about 12. The absolute accuracy of our measurements of the line positions are, therefore, about ± 0.002 cm^{-1} for strong unblended lines.

OBSERVATION AND ANALYSIS

The interferograms were transformed by G. Ladd of the National Solar Observatory to provide the spectra. The line positions of the CrH molecule were measured using a data reduction program called PC-DECOMP, developed by J. Brault at the National Solar Observatory. To find the line positions, a Voigt lineshape function was fitted to the CrH lines.

Our observed spectrum consists of a 0 − 0 vibrational band of moderate intensity and very weak 0 − 1, 1 − 1, and 1 − 0 bands. We did not attempt, therefore, to analyze the 0 − 1, 1 − 1, and 1 − 0 bands. Cr has four naturally occurring isotopes, ^{50}Cr, ^{52}Cr, ^{53}Cr, and ^{54}Cr, with abundances of 4.8, 83.8, 9.5, and 2.4%, respectively. The minor isotopic species were not observed and the data reported in this paper are for the ^{52}CrH isotopomer.

As observed by Kleman and Uhler (*5*) the spectrum consists of six R and six P branches consistent with a $^6\Sigma^+ - ^6\Sigma^+$ assignment. The connecting R and P branches

TABLE II—*Continued*

N	R4	O-C		P4	O-C		R5	O-C		P5	O-C		R6	O-C		P6	O-C	
2	11573.104	6																
3	11578.438	6																
4	11581.767	-1		11486.751	8		11572.416	2					11563.636	-14				
5	11583.247	-2		11468.088	2		11572.870	-2		11459.663	4		11562.759	-2		11452.608	-9	
6	11582.935	-3		11447.237	-1		11571.487	-6		11437.928	5		11560.091	-2		11429.347	-8	
7	11580.873	-1		11424.552	-1		11568.331	-3		11414.231	-2		11555.686	-1		11404.282	-2	
8	11577.082	2		11400.156	-2		11563.438	2		11388.775	-3		11549.576	3		11377.521	-1	
9	11571.567	-12	*	11374.121	-0		11556.827	1		11361.653	-1		11541.775	0		11349.136	-2	
10	11564.402	13	*	11346.489	1		11548.538	10	*	11332.918	-2		11532.315	1		11319.184	2	
11	11555.568	37	*	11317.311	11	*	11538.603	38	*	11302.632	5		11521.215	1		11287.700	5	
12	11545.090	66	*	11286.612	19	*	11527.021	60	*	11270.829	14	*	11508.497	3		11254.720	3	
13	11533.011	120	*	11254.442	37	*	11513.850	111	*	11237.556	32	*	11494.183	2		11220.286	2	
14	11519.362	204	*	11220.842	71	*	11499.113	190	*	11202.858	65	*	11478.291	-6		11184.438	2	
15	11504.200	352	*	11185.852	124	*	11482.856	316	*	11166.776	114	*	11460.876	6		11147.211	0	
16	11487.595	607	*	11149.526	209	*	11465.147	531	*	11129.361	191	*	11441.928	-1		11108.649	-0	
17	11469.733	1124	*	11111.935	357	*	11446.109	928	*	11090.675	317	*	11421.505	4		11068.789	-3	
18	11451.161	2422	*	11073.160	608	*	11426.170	1905	*	11050.798	530	*	11399.620	1		11027.679	-4	
19	11435.117	7704	*	11033.404	1120	*	11407.718	5818	*	11009.878	935	*	11376.319	3		10985.360	-4	
20	11399.248	-5417	*	10993.233	2418	*	11373.609	-4511	*	10968.330	1902	*	11351.622	-6		10941.875	-7	
21	11377.318	-3212	*	10955.899	7704	*	11350.648	-2313	*	10928.579	5812	*	11325.597	7		10897.281	-3	
22	11352.602	-2445	*	10899.049	-5419	*	11324.898	-1562	*	10873.502	-4507	*	11298.260	19		10851.614	-2	
23	11326.109	-2147	*	10856.471	-3214	*	11297.445	-1214	*	10829.892	-2310	*	11269.627	3		10804.944	15	
24	11298.260	-1940	*	10811.408	-2490	*	11268.651	-945	*	10783.806	-1590	*				10757.272	-2	
25	11269.025	-1898	*	10765.004	-2153	*	11238.617	-702	*	10736.433	-1210	*				10708.708	4	
26	11238.749	-1723	*	10717.542	-1974	*				10688.030	-965	*				10659.277	3	
27				10669.144	-1888	*				10638.743	-767	*				10609.034	-5	
28				10620.006	-1755	*				10588.629	-613	*						
29				10569.919	-1844	*				10537.798	-454	*						
30				10519.109	-1989	*												

TABLE III

Hyperfine-Free Pure Rotational Transitions of CrH (in cm^{-1})

N'-N"	J'-J"	Wavenumber	O-C
1-0	1.5-2.5	11.249723	72
	2.5-2.5	13.228125	-10
	3.5-2.5	12.095851	23
2-1	2.5-1.5	25.887179	50
	3.5-2.5	24.353728	4
	4.5-3.5	24.515310	41
3-2	1.5-0.5	37.240863	22
	2.5-1.5	37.224809	57
	3.5-2.5	36.936736	-30
	4.5-3.5	36.697184	47
	5.5-4.5	36.807861	21
4-3	1.5-0.5	48.974097	20
	2.5-1.5	49.131299	31
	3.5-2.5	49.129672	-77
	4.5-3.5	49.031617	-63
	5.5-4.5	48.956752	60
	6.5-5.5	49.045076	-34
5-4	2.5-1.5	61.092768	-7
	3.5-2.5	61.201123	-61
	4.5-3.5	61.216176	-203
	5.5-4.5	61.180415	-110
	6.5-5.5	61.160655	51
	7.5-6.5	61.237128	-120

O-C: Observed minus calculated line positions in 10-6 cm-1.

TABLE IV

Spectroscopic Constants for CrH (cm^{-1})

	$A\,^6\Sigma^+$	$X\,^6\Sigma^+$	$X\,^6\Sigma^{+a}$
E	11552.6848(10)		
B	5.271996(29)	6.1317406(19)	6.1317456(11)
$D\times10^{4}$	2.5477(20)	3.48946(29)	3.4951(34)
$H\times10^{8}$	0.508(40)	1.2497(33)	1.59(FIXED)
$L\times10^{12}$	2.03(25)		
γ	1.30211(11)	0.0503580(70)	0.0503323(18)
$\gamma_D\times10^{4}$	-1.5438(93)	-0.02750(89)	0.03451(81)
$\gamma_H\times10^{8}$	8.29(31)		
$\gamma_L\times10^{11}$	-2.64(24)		
λ	1.57598(32)	0.2328209(56)	0.2328341(17)
$\lambda_D\times10^{4}$	-8.484(67)	-0.0954(61)	0.09831(21)
$\Theta\times10^{3}$	2.75(21)	-0.0785(29)	-0.0773(10)
$\Theta_D\times10^{4}$	-1.001(40)		
$\gamma_S\times10^{4}$	8.84(18)	0.0474(91)	
$\gamma_{SD}\times10^{6}$	6.58(28)		
$b_F\times10^{3}$			-1.1607(67)
$c\times10^{3}$			1.395(21)

[a]: constants from LMR work of reference 9.

were picked out using an interactive color Loomis–Wood program running on a 486/33 microcomputer. The assignment of the different branches was obtained using the previous work of Kleman and Uhler (*5*) and also the ground state combination differences obtained from the pure rotational spectra (*9*).

As first observed by Kleman and Uhler (*5*), the spectra are affected by several perturbations. Our observations show that F_1, F_2, and F_3 spin components are locally perturbed between $N = 9$ and $N = 10$ in the excited state, whereas F_2, F_3, F_4, and F_5 spin components are strongly perturbed between $N = 20$ and 21. The F_6 spin component is unperturbed. Our results are in contrast to those of Kleman and Uhler (*5*) who concluded that all six components were perturbed between $N = 20$ and $N = 21$. Our present observations lead us to conclude that a nearby $^4\Sigma^+$ excited state is responsible for these perturbations.

A part of the spectrum of the $0 - 0$ band near the bandhead is presented in Fig. 1. The observed wavenumbers were fitted with the usual N^2 Hamiltonian for a $^6\Sigma$ state as given by Brown and Milton (*23*). An explicit listing of most of the necessary matrix elements is given by Gordon and Merer (*24*). Some additional matrix elements such as for H, L, γ_H, and γ_L were derived by matrix multiplication and the complete Hamiltonian matrix used is provided in Table I. Because of the presence of extensive perturbations in the excited state we could not, at first, determine reliable values for rotational constants for the ground state from a free fit of our observed lines. To avoid the effects of the perturbation in the final fit we therefore included only the unperturbed transition wavenumbers and the ground state combination differences corresponding to the perturbed transitions together with the hyperfine-free pure rotational transitions

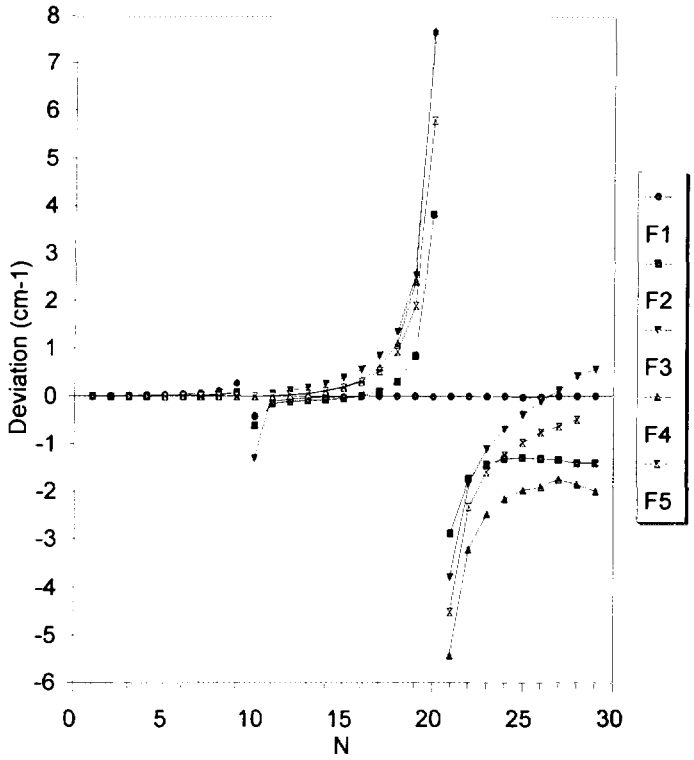

FIG. 2. The deviations of the observed line positions of CrH from the calculated line positions (calculated with the constants of Table IV) are plotted as a function of N'. The perturbations in $v = 0$ of the $A^6\Sigma^+$ state between $N' = 9$ and $N' = 10$ for F_1, F_2, and F_3 and $N' = 20$ and $N' = 21$ for F_2, F_3, F_4, and F_5 are evident in the plot.

from Brown (*25*). The perturbed transitions were excluded from the fit. The observed transition wavenumbers of the 0 − 0 band are listed in Table II and the hyperfine-free pure rotational transitions are given in Table III. In the final fit the molecular parameters B, D, H, γ, γ_D, γ_S, λ, λ_D, and θ for the ground state and T_0, B, D, H, L, γ, γ_D, γ_H, γ_L, γ_S, γ_{SD}, λ, λ_D, θ, and θ_D for the excited state were required in order to obtain a satisfactory fit. The final constants obtained for the ground and excited states are provided in Table IV where the laser magnetic resonance constants from Corkery *et al.* (*9*) have also been listed for comparison.

DISCUSSION

The ground state of CrH is well characterized by precise laser magnetic resonance measurements. However, the combination of the very precise (1 MHz) pure rotational transitions for the lower N transitions ($1 \leftarrow 0$ to $5 \leftarrow 4$) with our combination differences for the high N transitions (up to $N'' = 28$) provides an improved set of constants for $v = 0$. As can be seen in Table IV our constants are generally in agreement with those of Corkery *et al.* (*9*). Note that the signs of λ_D and γ_D need to be changed in the paper by Corkery *et al.* (9, 25)

The ground state of CrH arises by combining a Cr atom with a high-spin $4s^1\ 3d^5$ configuration with a H atom ($1s^1$). The ab initio calculations show that the $4s^2\ 3d^4$

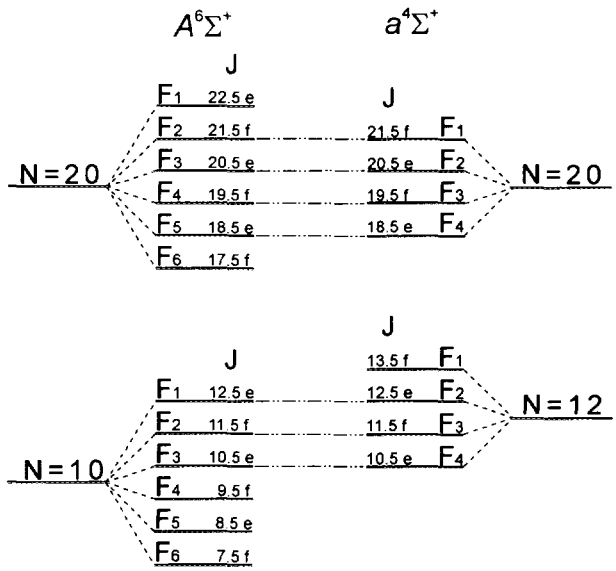

FIG. 3. The $\Delta N = 0$ (top) and $\Delta N = 2$ (bottom) interactions between a $^6\Sigma^+$ state and a $^4\Sigma^+$ state are depicted.

Cr atomic configuration contributes little to the formation of the bond (*15*). The lowest energy molecular configuration is $(1\sigma)^2(2\sigma)^1(1\delta)^2(1\pi)^2$, where the 1σ and 2σ orbitals are mixtures of Cr($4s\sigma$), Cr($3d\sigma$), and H($1s\sigma$) atomic orbitals, while the 1δ and 1π are Cr($3d\delta$) and Cr($3d\pi$) atomic orbitals. The excited $A^6\Sigma^+$ state is derived from the excited configuration $(1\sigma)^1(2\sigma)^2(1\delta)^2(1\pi)^2$ obtained by simple promotion of one electron from the 1σ orbital to the 2σ orbital in the lowest energy configuration.

Consideration of the molecular states correlating with separated atoms is also helpful. The combination of a ground state ^7S Cr atom with a ^2S H atom gives rise to $^6\Sigma^+$ and $^8\Sigma^+$ CrH molecular states. It is likely that the $^8\Sigma^+$ state is a repulsive state since the necessary molecular configuration involves promotion of a bonding 1σ electron to an antibonding σ^* orbital $[(1\sigma)^1(2\sigma)^1(1\delta)^2(1\pi)^2(3\sigma^*)^1]$.

Another $^6\Sigma^+$ state and a $^4\Sigma^+$ state can be derived by combining an excited ^5S Cr atomic state at 7593 cm^{-1} from the same $4s^1\,3d^5$ configuration with the ^2S H atom. In this case the corresponding molecular configurations are $(1\sigma)^1(2\sigma)^2(1\delta)^2(1\pi)^2$ for the $^6\Sigma^+$ state and $(1\sigma)^2(2\sigma)^1(1\delta)^2(1\pi)^2$ for the $^4\Sigma^+$ state. These states are the $A^6\Sigma^+$ and $a^4\Sigma^+$ states of CrH.

The most interesting result of our reanalysis of the $A^6\Sigma^+$–$X^6\Sigma^+$ transition is the interpretation of the perturbations observed in the $A^6\Sigma^+$ state. Kleman and Uhler (*5*) claimed to have observed perturbations in all six spin components with the crossing occurring occurring between $N = 20$ and $N = 21$. This led them to conclude that the perturbing state was an $^8\Sigma^+$ state. Since the $^8\Sigma^+$ state is probably repulsive, this seems unlikely.

In contrast we find that the F_1 and F_6 spin components are not perturbed near $N = 20$ and 21 (Fig. 2). The perturbation selection rules are $\Delta J = 0$ with $e \leftrightarrow e$ and $f \leftrightarrow f$ because J and parity are always good quantum "numbers" for a diatomic molecule. Since the perturbation occurs at the same N for four different J values, the

perturbing state must have four nearly degenerate spin components. The only possible perturbing state consistent with this observation is a $^4\Sigma^+$ state (Fig. 3).

The interaction of a $^6\Sigma^+$ state and a $^4\Sigma^+$ state occurs through the microscopic form of the spin–spin operator (*26*). The additional selection rules $\Delta N = 0$, 2, and 4 are obtained by considering the energy level pattern of the $^6\Sigma^+$ and $^4\Sigma^+$ states and the selection rules on J and parity.

The perturbation which culminates between $N = 9$ and $N = 10$ for the F_1, F_2, and F_3 spin components confirms our assignment of the perturber and allows the estimation of the molecular parameters. These low N perturbations are also much weaker than those at $N = 20$. These observations are consistent with a $\Delta N = 2$ interaction with a $^4\Sigma^+$ state. In this case the F_1, F_2, and F_3 spin components of the $^6\Sigma^+$ state interact with the F_2, F_3, and F_4 spin components of the $^4\Sigma^+$ state (Fig. 3).

Spectroscopic constants can be estimated from the perturbations at $N = 10$ and 21 of $v = 0$ of the $A^6\Sigma^+$ state of CrH. Using the simple energy level expression $F(N) = B_pN(N + 1) - D_p[N(N + 1)]^2$, with $D_p = 3.3 \times 10^{-4}$ for the perturbing state, we calculate $B_p = 6.10$ cm^{-1}. The origin (T_0) of the perturbing $^4\Sigma^+$ state is at about 11 186 cm^{-1}. These are simple preliminary estimates of uncertain reliability. In the future we plan to analyze the spectrum of CrD, also recorded with the McMath Fourier transform spectrometer, and we will undertake a thorough deperturbation of the $A^6\Sigma^+$ state for both CrH and CrD.

Since the origin of the perturbing state lies about 366 cm^{-1} below the origin of the $A^6\Sigma^+$ state (Table IV), the $a^4\Sigma^+$ state is the lowest known excited state of CrH. The vibrational assignment of the perturbing state can be made from several pieces of evidence. The perturbation at $N = 21$ is very strong, suggesting a $\Delta v = 0$ interaction. The $A^6\Sigma^+$ and $a^4\Sigma^+$ states have similar rotational constants so that a $\Delta v \neq 0$ matrix element would be small because of the small vibrational overlap factor (*26*). The photoelectron spectrum of CrH^- is also consistent with a $\Delta v = 0$ interaction. The unassigned peak, labeled "A" by Miller *et al.* (*17*), is located at about 11 200 cm^{-1}, consistent with the assignment of this peak to $v = 0$ of the $a^4\Sigma^+$ state. Unfortunately these authors neglected to quote the actual position of peak A in their paper.

The most convincing evidence for the vibrational assignment of $v = 0$ for the perturber and for our estimated constants comes from the analysis of the 0 – 0 band of CrD. O'Connor (*6*) found the F_1, F_2, and F_3 spin components of the $A^6\Sigma^+$ states perturbed at $N = 18$, consistent with a $\Delta N = 2$ interaction with $N = 20$ of the $a^4\Sigma^+$ state. The energy level expression $F(N) = 3.106\ N(N + 1) - 8.6 \times 10^{-5}\ [N(N + 1)]^2$ was estimated from CrH using isotopic relationships (*27*). This energy level expression predicts a band origin (T_0) of 11 198 cm^{-1} for the $a^4\Sigma^+$ state of CrD. This value is very similar to the origin determined for the perturbing state of CrH and confirms both the vibrational assignment and our preliminary perturbation analysis.

The rotational constant B_p ($v = 0$) = 6.10 cm^{-1} for the $a^4\Sigma^+$ state is very similar to the ground state value of B'' = 6.1317 cm^{-1}, as expected, since both states arise from the same $(1\sigma)^2\ (2\sigma)^1\ (1\delta)^2\ (1\pi)^2$ configuration. The value of the rotational constant of the perturbing state is greater than the value of the $A^6\Sigma^+$ ($B_p > B'$) since the perturbing state crosses from below (Fig. 2).

The ab initio calculations of Dai and Balasubramanian (*21*) are very useful for supporting some of the conclusions of our study and suggest that there may be additional nearby low-lying electronic states. Dai and Balusubramanian (*21*) calculate that the $^8\Sigma^+$ state, which correlates to the $Cr(^7S) + H(^2S)$ atomic limit, is repulsive, as expected. In addition they predict a low-lying $^4\Sigma^+$ excited state at 11 206 cm^{-1} with

a bond length r_e = 1.693 Å. This is in excellent agreement with our values of T_{00} = 11 186 cm^{-1} and r_0 = 1.672 Å. The $A^6\Sigma^+$ state is predicted (*21*) to lie at T_e = 12 834 cm^{-1}, compared to our observed value of T_{00} = 11 552.68 cm^{-1}. The calculations also confirm that, as expected on the basis of the atomic limits, there are no additional states lying between the $A^6\Sigma^+$, $a^4\Sigma^+$ pair of states and the ground $X^6\Sigma^+$ state.

CONCLUSION

The 0 − 0 band of the $A^6\Sigma^+$–$X^6\Sigma^+$ transition of CrH was reanalyzed. The spectrum was recorded in the near-infrared in emissions from a hollow cathode lamp. Improved molecular constants were determined for the $A^6\Sigma^+$ and $X^6\Sigma^+$ states. The perturbations observed in the $A^6\Sigma^+$ are consistent with the presence of the $a^4\Sigma^+$ state below the A state. Preliminary spectroscopic constants were estimated for this new state.

ACKNOWLEDGMENTS

We thank J. Wagner, C. Plymate, and G. Ladd for assistance in obtaining the spectra at Kitt Peak. The National Solar Observatory is operated by the Association of Universities for Research in Astronomy, Inc., under contract with the National Science Foundation. We thank J. Brown for calculating the hyperfine-corrected transitions listed in Table III. We thank K. Balsubramanian for undertaking ab initio calculations on CrH and providing the results in advance of publication. Acknowledgment is made to the donors of the Petroleum Research Fund, administered by the American Chemical Society, for partial support of this work. Support was also provided by the Centre of Excellence in Molecular and Interfacial Dynamics (CEMAID) and the NASA Origin of the Solar System Program.

RECEIVED: May 10, 1993

REFERENCES

1. A. G. GAYDON AND R. W. B. PEARSE, *Nature* **140,** 110 (1937).
2. S. O'CONNOR, *J. Phys. B* **2,** 541–543 (1969).
3. R. E. SMITH, *Proc. R. Soc. London A* **332,** 113–127 (1973).
4. B. KLEMAN AND B. LILJEQVIST, *Ark. F. Fysik* **9,** 345–347 (1955).
5. B. KLEMAN AND U. UHLER, *Can. J. Phys.* **37,** 537–549 (1959).
6. S. O'CONNOR, *Proc. R. Irish Acad. A* **65,** 95–111 (1967).
7. R. J. VAN ZEE, T. C. DEVORE, AND W. WELTNER, JR., *J. Chem. Phys.* **71,** 2051–2056 (1979).
8. R. J. VAN ZEE, C. A. BAUMANN, AND W. WELTNER, JR., *Chem. Phys. Lett.* **113,** 524–529 (1985).
9. S. M. CORKERY, J. M. BROWN, S. P. BEATON, AND K. M. EVENSON, *J. Mol. Spectrosc.* **149,** 257–273 (1991).
10. K. LIPUS, E. BACHEM, AND W. URBAN, *Mol. Phys.* **73,** 1041–1050 (1991).
11. A. KANT AND K. A. MOON, *High Temp. Sci.* **14,** 23–31 (1981).
12. L. SALLANS, K. R. LANE, R. R. SQUIRES, AND B. S. FREISER, *J. Am. Chem. Soc.* **107,** 4379–4385 (1985).
13. Y.-M. CHEN, D. E. CLEMMER, AND P. B. ARMENTROUT, *J. Chem. Phys.* **98,** 4929–4936 (1993).
14. G. DAS, *J. Chem. Phys.* **74,** 5766–5774 (1981).
15. S. P. WALCH AND C. W. BAUSCHLICHER, *J. Chem. Phys.* **78,** 4597–4605 (1983).
16. D. P. CHONG, S. R. LANGHOFF, C. W. BAUSCHLICHER, S. P. WALCH, AND H. PARTRIDGE, *J. Chem. Phys.* **85,** 2850–2860 (1986).
17. A. E. S. MILLER, C. S. FEIGERLE, AND W. C. LINEBERGER, *J. Chem. Phys.* **87,** 1549–1556 (1987).
18. J.-S. LIN AND J. V. ORTIZ, *Chem. Phys. Lett.* **171,** 197–200 (1990).
19. O. ENGVOLD, H. WÖHL, AND J. W. BRAULT, *Astron. Astrophys. Suppl. Ser.* **42,** 209–213 (1980).
20. B. LINDGREN AND G. S. OLOFSSON, *Astron. Astrophys.* **84,** 300–303 (1980).
21. D. DAI AND K. BALASUBRAMANIAN, *J. Mol. Spectrosc.* **161,** 455–465 (1993).
22. B. A. PALMER AND R. ENGLEMAN, "Atlas of the Thorium Spectrum," unpublished, Los Alamos National Laboratory, Los Alamos, 1983.
23. J. M. BROWN AND D. J. MILTON, *Mol. Phys.* **31,** 409–422 (1978).
24. R. M. GORDON AND A. J. MERER, *Can. J. Phys.* **56,** 642–656 (1980).
25. J. M. BROWN, private communication.
26. H. LEFEBVRE-BRION AND R. W. FIELD, "Perturbations in the Spectra of Diatomic Molecules." Academic Press, Orlando, 1986.
27. G. HERZBERG, "Spectra of Diatomic Molecules," Van Nostrand, New York, 1950.